Journal of the European Ceramic Society 21 (2001) 765–777

www.elsevier.com/locate/jeurceramsoc

On the transformation toughening of Y–ZrO_2 ceramics with mixed Y–TZP/PSZ microstructures

D. Casellas [a,*], F.L. Cumbrera [b], F. Sánchez-Bajo [c], W. Forsling [d], L. Llanes [a], M. Anglada [a]

[a] *Departamento de Ciència dels Materials i Enginyeria Metal.lúrgica, Universitat Politècnica de Catalunya, ETSEIB., Avda. Diagonal 647, 08028 Barcelona, Spain*

[b] *Departamento de Física, Facultad de Ciencias, Universidad de Extremadura, Avda. de Elvas s/n., 06071 Badajoz, Spain*

[c] *Departamento de Electrónica e Ingeniería Electromecánica, ETSII, Universidad de Extremadura, Avda. de Elvas s/n., 06071 Badajoz, Spain*

[d] *Department of Inorganic Chemistry, Luleå University of Technology, S-97187 Luleå, Sweden*

Received 27 April 2000; received in revised form 4 September 2000; accepted 21 September 2000

Abstract

Heat treatment of Y–TZP at high temperatures produces materials with a mixed Y–TZP/PSZ phase assemblage, which exhibit a unique combination of high mechanical strength and fracture toughness, uncommon in zirconia ceramics. The microstructure and crack growth resistance of the Y–TZP/PSZ materials developed by treating at 1650°C in air a fine-grained Y–TZP was studied. XRD as well as Raman spectroscopy results indicate that the obtained microstructure allow the retention of large tetragonal grains (up to ~4 μm), resulting in both phase transformability enhancement and pronounced R-curve behavior. The large transformation zone, discerned from accurate measurements with Raman microprobe spectroscopy, sustains the above assessment and points out tetragonal to monoclinic phase transformation as the main toughening mechanism in the investigated Y–TZP/PSZ microstructures. This was confirmed by satisfactory agreement between the transformation toughening estimated from numerical analysis and the crack shielding experimentally determined from the R-curve measurements.

Keywords: Crack growth; Mechanical properties; Phase transformations; R-curve; Toughness and toughening; ZrO_2

1. Introduction

The outstanding toughening capability exhibited by zirconia-based ceramics has raised considerable attention in these materials as potential candidates for structural applications. The source for achieving such relatively high fracture toughness is the stress-driven phase transformation that tetragonal (t) zirconia undergoes to monoclinic (m) symmetry.[1–3] This tetragonal to monoclinic (t→m) transformation is martensitic, and results in a volume increase, which induces compressive stresses around propagating cracks. From a toughening viewpoint, an interesting issue is that transformation extent may be enhanced by tailoring microstructural parameters such as grain size or phase assemblage[4–10] as well as chemical composition.[9,10]

Following the above ideas, in the last two decades different zirconia-toughened ceramics (ZTC) have been developed aiming to improve the fracture toughness of these materials. Thus, addition of different stabilizing oxides (Y_2O_3, MgO and CeO_2 among others), has been used to retain metastable tetragonal zirconia at room temperature. As a result, two ZTCs are now extensively applied: MgO–ZrO_2, usually referred to as Mg–PSZ (magnesia–partially-stabilized-zirconia), and Y_2O_3–ZrO_2, commonly named Y–TZP (yttria–tetragonal zirconia polycrystals).

The Mg–PSZs contain a considerable amount of stabilizer (6–10 mol%) and are conventionally sintered at high temperatures (1700–1800°C) followed by aging treatments at temperatures around 1400°C. The resulting microstructure may be described as consisting of submicron tetragonal precipitates embedded within

* Corresponding author at Centre Tecnològic de Manresa, Avda Bases de Manresa 1,08240 Manresa, Spain. Tel.: +34-3-874-8730; fax: +34-3-874-8731.

0955-2219/01/$ - see front matter
PII: S0955-2219(00)00273-9

cubic grains of about 50 μm in size. The extensive t→m transformation of the former is responsible for the high fracture toughness (> 10 MPa$\sqrt{m}$) that these materials exhibit, whereas the large grain size of the latter is indirectly accountable for their moderate fracture strength (about 500 MPa).[4]

On the other hand, the Y–TZPs are stabilized through a small amount of yttria (about 2.5 mol%) allowing to attain fully tetragonal grains at sintering temperatures between 1400 and 1550°C. The resulting fine-grained microstructures yield very high fracture strength (> 1 GPa), although related to low fracture toughness values (between 4 and 5 MPa$\sqrt{m}$).[4]

Although the aforementioned inverse correlation between fracture toughness and flexural strength is typical for zirconia ceramics, recent results on Y–TZP heat treated at high temperatures (1650–1750°C) point out that ZTCs combining high fracture toughness and strength may be developed.[11] In the Y_2O_3–ZrO_2 system and for small contents of stabilizer, the wide cubic and tetragonal phase field[12] permits to develop a complex aggregate consisting of grains with features close to PSZ in addition to tetragonal grains larger than those characteristic of Y–TZP.[13,14] Such materials with a mixed Y–TZP/PSZ microstructure posses not only a fracture toughness close to that commonly found for Mg–PSZ, but also fracture strength values similar to those of Y–TZP, despite of the clear increase in grain size. This attractive combination of mechanical properties allows to consider these Y–TZP/PSZ materials as candidates for structural applications. In this sense, a more complete understanding of the relationships between mechanical properties and microstructure in these Y–TZP/PSZ materials seems to be required if they are to be used effectively.

In an effort to address the above issue, the aim of this paper is to study the toughening phenomena associated with Y–TZP/PSZ materials obtained by heat treatment at 1650°C of an originally fine-grained Y–TZP. In doing so, Raman microprobe spectroscopy is used as experimental technique to estimate the extension of the t→m transformation. Such a technique has proven to be very useful in previous studies about toughening of ZTC,[15–18] particularly because of its ability of clearly discerning the existence of monoclinic phase promoted by such transformation as well as its accurate high spatial resolution in terms of scanning through very reduced zones of the material. The results obtained with Raman spectroscopy will allow to determine the height of the transformed zone as well as permit to estimate the role of transformation toughening as operating mechanism for improving the fracture resistance of these materials. These results will be compared with R-curve experiments, conducted in a previous work,[19] and will be discussed in terms of the microstructural changes and toughening mechanisms.

2. Experimental procedure

Yttria-stabilized zirconia-based ceramics with three distinct microstructures were studied. Microstructural differences, given in terms of grain size and phase distribution, were induced by heat treating a fine-grained Y–TZP at 1650°C in air during 2 and 10 h. In this study, the resulting microstructures are referred to as 2H and 10H respectively. The stabilizers used were yttria (2.5 mol%) and hafnia (1.0 mol%), while magnesia is the major impurity (0.06 mol%).

Grain size (d) was determined through scanning electron microscopy (SEM) examination of polished and thermally etched (1450°C for 30 min) surfaces. It is described by the spherical equivalent diameter. Phase assemblage was discerned using transmission electron microscopy (TEM). In doing so, phase identification (crystal symmetry) was performed through analysis of electron diffraction patterns of substructural features with quite distinct aspects. Quantitative distribution of monoclinic, tetragonal and cubic phases was determined by X-ray diffraction (XRD) in polished as well as fracture surfaces. The monoclinic amount in the fracture surfaces (V_F) was related to the extension of stress-induced phase transformation. Phase recognition was made by Rietviled analysis of XRD data; microstructural effects such as preferred orientation and anisotropic line broadening were considered not only for improving the refining but also for determining the accurate proportion of the existing phases. The experimental details of the XRD analysis performed have been reported elsewhere.[20]

The degree of transformation toughening was evaluated by Raman spectroscopy. This technique is particularly suitable for identification of monoclinic and tetragonal phases in zirconia materials because the wide separation between the corresponding characteristic lines: the monoclinic doublet at 181 and 192 cm^{-1} and the tetragonal bands at 148 and 264 cm^{-1}.[15–17] On the other hand, cubic lines are not readily discerned in a mixed-phase sample because of their broadness.[17,18] The spectrometer used was a Renishaw Raman (system 2000) with a laser of 632.8 nm and joined to an optical microscope equipped with ultra-long focal lens. The shape of the analysis zone was circular with an approximate diameter of 2 μm. The penetration beam depth was about 1 μm.

The intensity of Raman bands is directly proportional to the concentration of scattering molecules; thus, a quantitative microanalysis of monoclinic and tetragonal phases may also be conducted. However, a calibration step is required because Raman intensities are affected by a number of factors, including incident laser power, frequency of the scattered radiation, absorptivity of the material and response of the detection system. This calibration procedure is based on XRD results and is

executed in order to convert spectral intensities into concentration of the above phases. Hence, monoclinic amount (V_m) may be expressed in terms of a function of the Raman intensities according to the relation:[17,18]

$$V_m = f\left(\frac{I_m^{181,192}}{I_t^{148} + I_t^{264} + I_m^{181,192}}\right) \quad (1)$$

The application of function f is required to convert Raman intensities into XRD ones. In this study, f was evaluated by equating the Raman intensities of the tetragonal phase and the Raman shifts determined in the fracture surface with the corresponding values obtained from XRD. Moreover, in order to obtain the f values for low and high concentration of monoclinic phase, two microstructures were prepared by mixing a known amount of monoclinic and tetragonal zirconia and sintering them at 1400°C for 2 h in air. The quantity of monoclinic phase in these materials was 5 and 50%.

Crack shielding due to phase transformation was evaluated from the measurement of the amount of monoclinic phase all around the crack propagation plane. In doing so, cracks were induced by applying a Vickers indenter on the polished surface. Spectra were taken at different positions along the crack length, as shown in Fig. 1: inside the indentation (⓪), at its corner (①), at half-length of the crack (②), and near (③) and in front of the crack tip (④). For each horizontal position, spectra were obtained at different distances along a direction perpendicular to the crack propagation plane, until the spectra matched that of the matrix, i.e. far away from the zone affected by the stress field associated with the crack. It allowed the evaluation of the maximum height of the process zone (h) due to phase transformation. The position for determining h was approximately at half-length of the total crack length ($\frac{1}{2}c_0$, in Fig. 1). Such a half way position between crack tip and indentation impression guarantees an h value exclusively associated with transformation toughening and eliminates the possible interference from the transformed zone generated around the indentation. Finally, the shape of the transformation zone, especially at the crack tip, was discerned by extrapolating the data obtained around indentation-induced cracks.

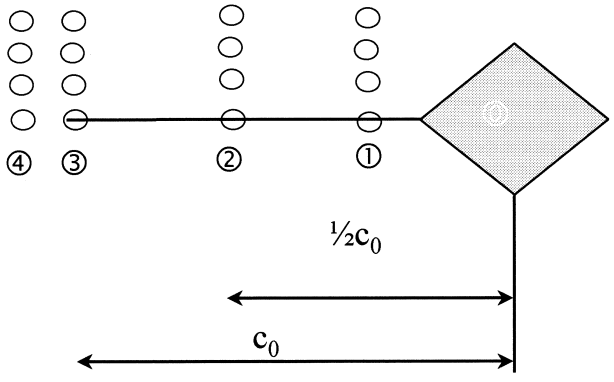

Fig. 1. Places analyzed by Raman spectroscopy around an indentation crack.

After the morphology of transformation zone has been fully determined, it is possible to estimate the transformation toughening levels. Such estimation is compared with the R-curve behavior of the studied microstructures, characterized in a previous work.[19] It is worth noting that this R-curve was determined with small semielliptical cracks. These cracks were obtained from indentation cracks, ground and polished to remove the central ligament and finally heat treated to transform the monoclinic phase induced in these steps back to the tetragonal symmetry. It results in a crack morphology close to those associated with natural preexisting flaws, and it is expected that the R-curve obtained from them would describe more precisely the shielding developed by the t→m transformation.

3. Results

3.1. Microstructural evolution

Heat treatment at 1650°C induced important microstructural changes (Table 1) in terms of grain size and volumetric fraction of cubic phase, of which the latter results from the equilibrium conditions at 1650°C dictated by the amount of stabilizer.[12] Before heat treatments (material Y–TZP), the microstructure was homogeneous with a very fine grain size [Fig. 2(a)]. However, heat treatment for 2 h produced a more heterogeneous microstructure, consisting of quite large grains surrounded by smaller ones [Fig. 2(b)]. On the other hand, the 10-h heat treatment resulted in a homogeneous microstructure, which is coarser than in Y–TZP and 2H materials [Fig. 2(c)]. Phase distribution from XRD analysis showed that the starting microstructure was initially fully tetragonal and the high temperature heat treatments promoted the formation of cubic phase (see Table 1). The amount of this phase did not reach the equilibrium value after 2 h of heat treatment

Table 1
Grain sizes and phase assemblage for the studied materials[a]

	d_{tg} (μm)	d_c (μm)	V_c	V_{tg}	V_{tp}
Y–TZP	0.3±0.01	–	0	1.0	0
2H	1.37±0.02	3.84±0.10	0.23	0.57	0.20
10H	2.33±0.05	4.63±0.08	0.37	0.31	0.32

[a] Microstructural dimensions are expressed in terms of tetragonal grain size (d_{tg}) and cubic grain size (d_c). The amount of each phase is given in terms of volumetric fraction of cubic grains (V_c), tetragonal precipitates (V_{tp}) and tetragonal grains (V_{tg}).

but went on growing, achieving a value close to the predictions at 1650°C from the phase diagram proposed by Scott, i.e. about 33%.[12]

In order to clearly determine the phase distribution of each microstructure, TEM examination, particularly in terms of electron diffraction, was focused to selected grains to obtain their crystallographic symmetry. It was confirmed that Y–TZP consists of tetragonal grains exclusively, but in the 2 h material the corresponding analysis allowed to discern that small grains were still tetragonal whereas large grains presented a tweed contrast. Such a contrast is usually associated with the presence of very small tetragonal precipitates formed by diffusional decomposition of the cubic matrix [Fig. 3(a)].[21,22] Tetragonal precipitates were detected using reflection in $\langle 111 \rangle_c$ plane, where the (112) cubic reflections are

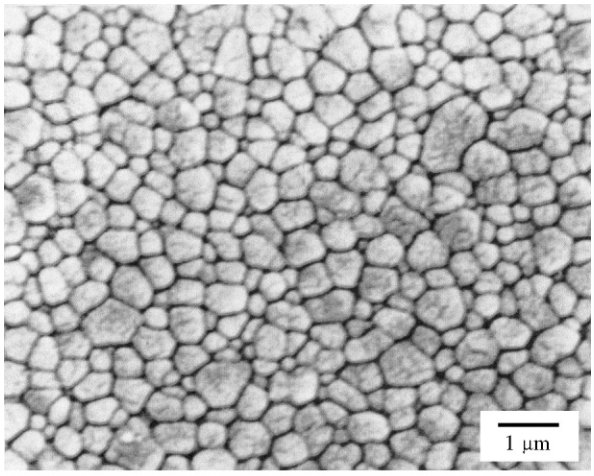

(a)

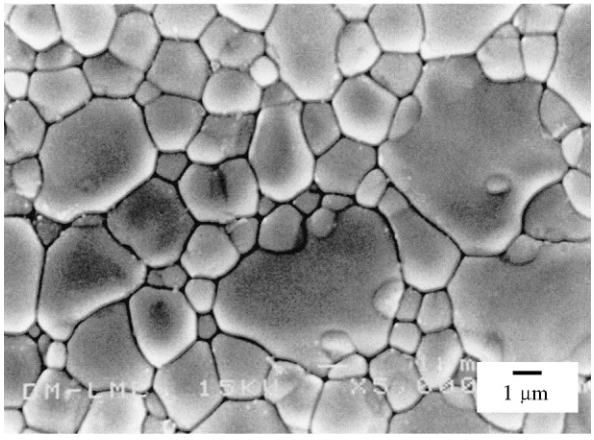

(b)

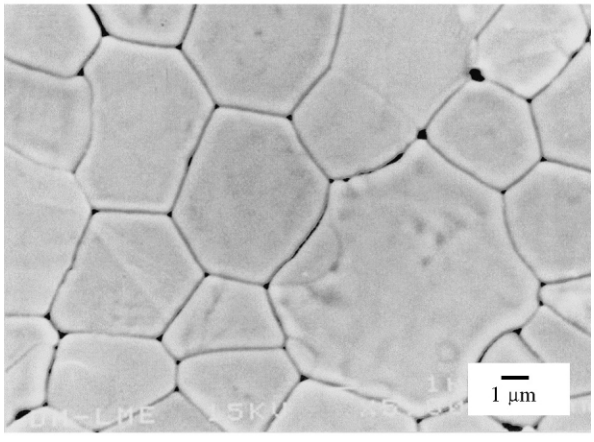

(c)

Fig. 2. SEM micrographs taken from the thermally etched surface of: (a) Y–TZP; (b) heterogeneous 2H microstructure, and (c) the coarse 10H microstructure.

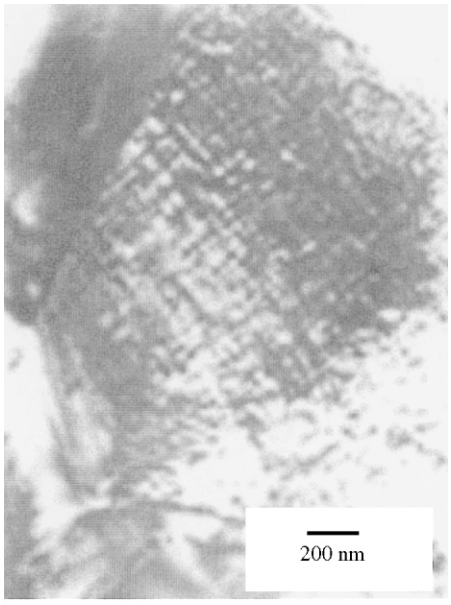

(a)

(b)

Fig. 3. (a) TEM micrograph showing the tweed contrast observed in cubic grains; (b) twinned grain in a 10H sample, due to the TEM preparation procedure.

forbidden and the $(112)_t$ can be distinguished. The presence of fine tetragonal precipitates has been reported in previous studies in yttria-stabilized zirconia sintered in the cubic-tetragonal field.[23,24] Qualitatively similar features were found in the 10H material, but here both tetragonal grains and precipitates coarsened. It is worthy to notice that neither the XRD nor the Raman spectroscopy results indicated the presence of monoclinic phase in the polished surfaces of 2H and 10H conditions. However, during TEM studies of 2H and 10H samples, in situ tetragonal to monoclinic transformation of several grains was observed, as a result of the electron beam incidence [Fig. 3(b)]. It was markedly pronounced for the 10H condition, as evidenced in several TEM samples that, after exposure to the electron beam, there were no tetragonal grains left, i.e. cubic grains were completely surrounded by monoclinic grains.

In the past, significant amounts of work aimed towards developing an understanding of the fundamental nature of microstructure-phase transformability correlation have been conducted.[6–10] As a result, it is now well-known that the chemical composition and tetragonal grain size dictate the phase transformation capability and determine the martensitic starting temperature (M_s). Such M_s value defines, for a given working temperature, a critical grain size (d_{CR}), beyond which any tetragonal grain will transform to monoclinic phase.[6–10] According to this, spontaneous phase transformation under electron beam of some tetragonal crystals should provide relevant information on the phase transformability of each studied microstructure. In this sense, the experimental findings referred to above allow speculation that heat treatments moved the grain size distribution closer to d_{CR}, inducing easier transformation of some grains. This seems to be especially true for 10H samples, where Raman and XRD results did not indicate any monoclinic phase at the polished surfaces, but after exposure to electron beam, all tetragonal grains had been transformed to the monoclinic symmetry.

Microstructural dimensions and phase amounts are shown in Table 1. Since the tetragonal phase is distributed as grains as well as fine precipitates, the XRD results can not discern between them. So, the phase assemblage is obtained by combining XRD results and stereologic studies. In doing so, the volumetric fraction of cubic phase (V_c) is assigned to the large grains clearly observed in 2H material. However, these grains contain tetragonal precipitates, which could not be detected from SEM observations. Hence, the volumetric fraction of the large grains is the sum of V_c and the volumetric fraction of the tetragonal precipitates (V_{tp}). Subtracting this V_{tp} of the tetragonal amount measured in XRD, yields the volumetric fraction of the free tetragonal crystals, i.e. the tetragonal grains (V_{tg}).

Based on all the above comments, the microstructural changes developed by heat treating a fine Y–TZP at 1650°C for 2 and 10 h, do not allow to describe the resulting material as a coarse-grained Y–TZP in a simple way. The presence of cubic grains with very fine tetragonal precipitates is a usual feature of PSZ materials. Thus, the obtained materials are more precisely referred to as yttria-stabilized ceramics with mixed Y–TZP/PSZ microstructures.

3.2. Raman calibration

The amount of the monoclinic phase determined by XRD was compared with the ratio between the intensity of the 181, 192 cm^{-1} monoclinic doublet ($I_m^{181,192}$) and the sum of this monoclinic intensity and the intensity of the 148 and 264 cm^{-1} tetragonal bands (I_t^{148} and I_t^{264}). In all cases, Raman intensities were obtained by subtracting the background and fitting them to the Pearson VII function. The results displayed a non-linear relationship (Fig. 4), which is in agreement with results obtained by Marshall et al. in Raman studies of a Mg–PSZ.[18] In other studies, it was assumed that such correlation is linear.[25,26] This assumption does not affect the determination of the transformation zone height, but influences the amount of monoclinic phase calculated within this zone and the corresponding shielding estimations. Taking this into consideration, a calibration curve that provides the value of V_m for a given Raman intensity ratio [Eq. (1)] was firstly obtained (Fig. 4). From this curve, an empirical equation between both variables was finally established:

$$V_m = 0.65 + 0.39\log\left(\frac{I_m^{181,192}}{+I_m^{181,192} + I_t^{148} + I_t^{264}}\right) \quad (2)$$

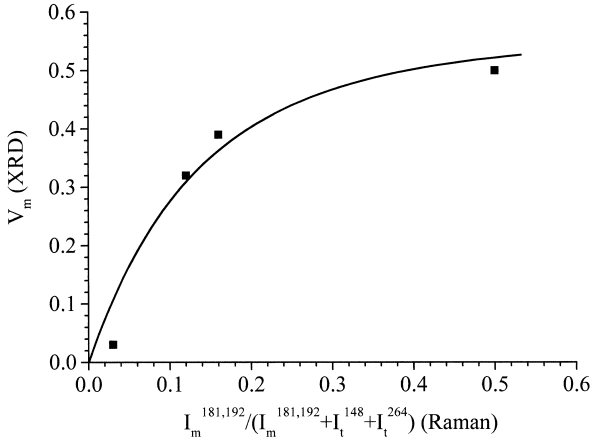

Fig. 4. Comparison of Raman intensity ratios with the monoclinic phase amount determined with XRD.

3.3. Fracture resistance and transformation toughening

Fracture and R-curve behavior of the different microstructures studied here have been published elsewhere.[19] The corresponding numerical results, in terms of flexural strength of cylindrical bars under three-point bending (σ_F), intrinsic crack propagation resistance of the material (K_0) and plateau toughness of the R-curve (K_R), are included in Table 2. In toughened ceramics, K_0 is defined as the fracture toughness of the material just to start crack extension when the crack is completely unshielded, i.e. without transformation zone, microcracked zone or crack bridging process zone. The difference between K_R and K_0 is the shielding due to the operating toughening mechanisms (K_S), i.e. stress-induced phase transformation, crack bridging, microcracking, etc. Thus, the fracture toughness (K_{IC}) of the material may be expressed as:

$$K_{IC} = K_0 + K_S \quad (3)$$

Also, for comparison with other materials, the fracture strength of prismatic bars under four-point bending, was estimated following the procedure exposed by Stanley et al.[27] From these fracture resistance properties, it is clear that heat treatment increases crack propagation resistance, by increasing both K_0 and K_S in 10H and 2H microstructures with respect to Y–TZP. It is worthy to note that here fracture toughness enhancement is not accompanied by a clear degradation of the fracture strength, since up most a decrease of about 10% is observed in 10H.

Raman spectra and XRD results pointed out that the three studied microstructures offer a different degree of transformation capability. Raman spectra obtained along crack flanks clearly showed that phase transformation around a propagating crack is more pronounced in coarser microstructures, developing large transformed zones around it (Figs. 5 and 6). The longer the heat treatment, the larger the corresponding transformation zone, as detailed in Table 3. These transformation zones surrounding the cracks are discerned using an optical microscope equipped with Nomarski interferometry, and are shown in Fig. 6. From this it may be confirmed that at half-length of the crack the value of h is not affected by the indentation impression, and corresponds to the maximum height of the zone, as assumed.

For the Y–TZP h was very small, which is characteristic of a very fine-grained Y–TZP with low phase transformation capability.[28] However, 2H and 10H microstructures have large values of h, close to those obtained in high-toughness zirconias.[5] With respect to the monoclinic amount in the fracture surface, it is also higher in 10H than in 2H (Table 3). These results, together with the above TEM observations (Section 3.1), clearly show that the microstructure achieved after 10 h of heat treatment at 1650°C exhibits a higher degree of phase transformability than that of the 2H material.

Once transformation height is obtained the amount of shielding developed by the t→m transformation may be evaluated if the transformation zone profile is known.[29] Hence, in order to obtain such estimation, the transformation zone morphology was determined through the Raman spectra. The obtained profiles are shown in Fig. 7, where a dark line is representing them. These profiles for the heat-treated microstructures were nearly

Table 2
Fracture resistance parameters of each microstructure determined from the R-curve measurements (K_0 and K_R), fracture strength (σ_F) of cylindrical rods under three-point bending and estimated fracture strength of prismatic bars under four-point bending (σ_F^*)

Material	K_0 (MPa$\sqrt{m}$)	K_R (MPa$\sqrt{m}$)	σ_F (MPa)	σ_F* (MPa)
Y–TZP	3.9	4.3	1076±90	860±72
2H	5.0±0.2	7.4±0.2	1058±80	867±66
10H	5.8±0.3	8.8±0.3	938±61	778±51

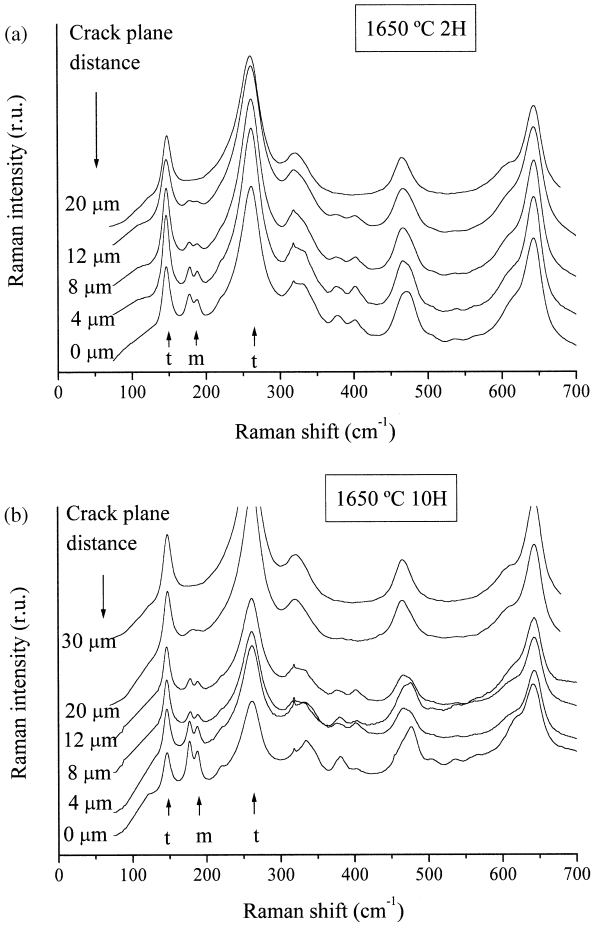

Fig. 5. Raman spectra obtained at $\frac{1}{2}c_0$ for Y–TZP/PSZ: (a) 2H, and (b) 10H. Peaks at 148 and 264 cm^{-1} are characteristics of the tetragonal phase. Doublet at 181 and 192 cm^{-1} reveals the existence of monoclinic phase.

semicircular, shape which is similar to that commonly found in high toughness Mg–PSZ.[18] The zone profile corresponding to fine-grained Y–TZP might not be evaluated because the transformation zone was too narrow.

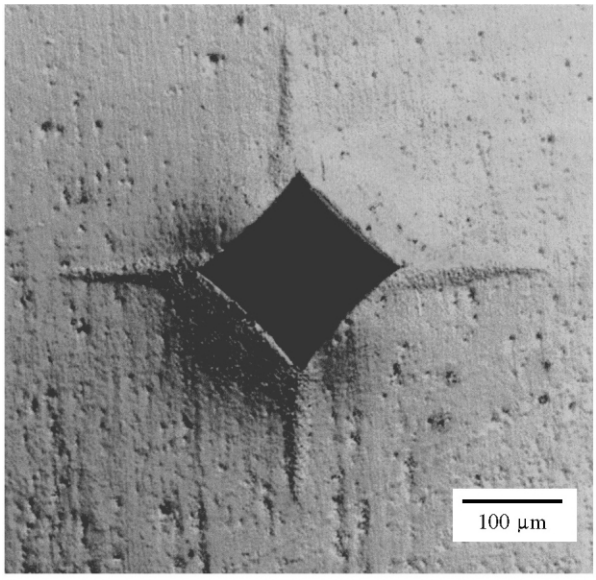

(a)

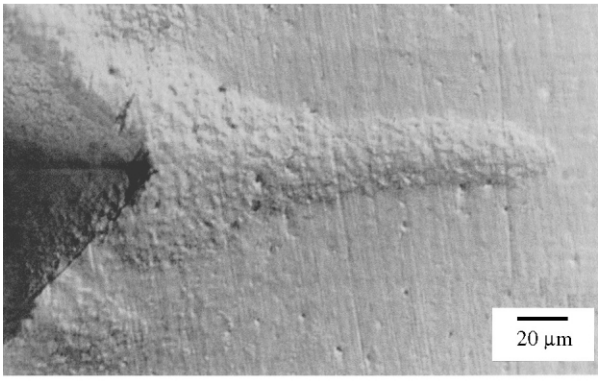

(b)

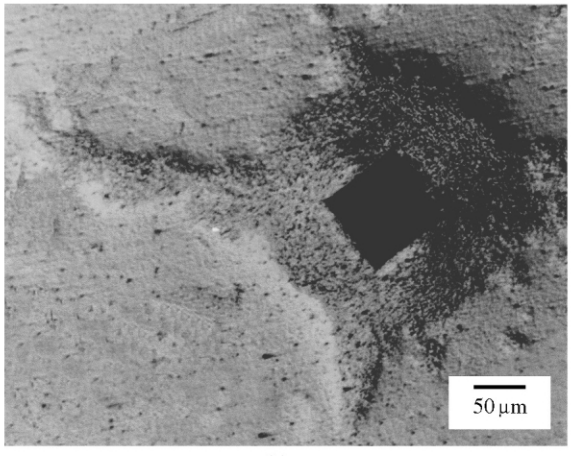

(c)

Fig. 6. Transformation zones around indentation cracks in Y–TZP/PSZ materials: (a) and (b) 2H, (c) 10H.

4. Discussion

The amount of the monoclinic phase at fracture surfaces, as well as the extension of t→m transformation, indicate that transformation toughening is the mechanism responsible for the increase in fracture toughness after heat treatment at 1650°C for different times. The high degree of transformation promotes a pronounced R-curve effect for 2H and 10H microstructures. In addition, the values given in Table 2 point out that the inferred microstructural changes increase the value of K_0 with respect to the initially fine-grained Y–TZP. Thus, the clear improvement of the fracture resistance induced by heat

Table 3
Monoclinic amount measured in fracture surfaces (V_F) and the values of transformed zone height (h)

Material	V_F	h (μm)
Y–TZP	0.05±0.03	2–3
2H	0.32±0.07	16±3
10H	0.39±0.05	28±5

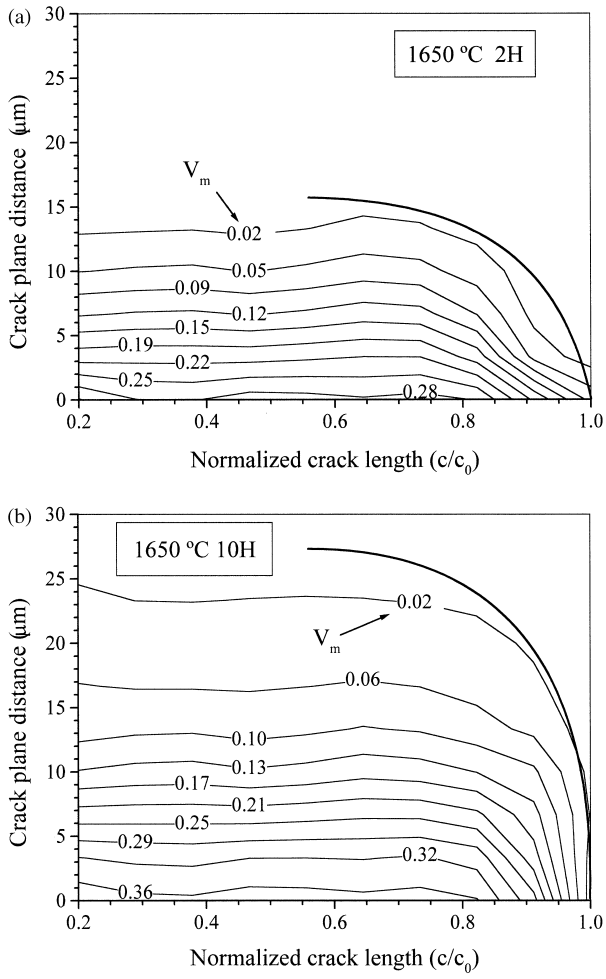

Fig. 7. Profile of the transformation zone in 2H and 10H. Numeric values correspond to V_m.

treatments should be rationalized by considering two different aspects: first, the increase in the intrinsic fracture resistance, and second, the large transformation capability that results in a raising R-curve behavior. Both phenomena are discussed separately and related to microstructural characteristics in the following sections.

4.1. Intrinsic fracture resistance

The value of K_0 calculated for Y–TZP is similar to that typically found for fine-grained Y–TZP.[30] Meanwhile the values obtained for 2H and 10H are markedly greater, and closer to the values reported for Mg–PSZ materials (ranging from 5 to 6 MPa$\sqrt{m}$).[5,31,32] Furthermore, the values of K_0 for 10H, a condition characterized by exhibiting a larger volumetric fraction of cubic grains with tetragonal precipitates than for 2H, were higher than those obtained for the latter material. Since the main difference in phase assemblage between Y–TZP and Y–TZP/PSZ is the presence of cubic phase grains with tetragonal precipitates, the observed increase in K_0 should be related to this microstructural feature. This assertion is supported by the work of Heuer et al.[21] and Michel et al.,[33] which found that the crack propagation resistance is enhanced in Y–PSZ single crystals compared to the cubic ones. For explaining such differences, they proposed some kind of crack-precipitate interaction to account for this precipitation toughening, because they were not able to discern any evidence for transformation toughening. In addition, Matsui et al. postulated that these precipitates increase transgranular strength in heat-treated Y–TZP with respect to materials before aging.[22]

In order to rationalize this increase in K_0, the intrinsic fracture resistance of each constituent, i.e. tetragonal grains and cubic grains with tetragonal precipitates, is considered. The K_0 value of the former may be considered to be the value obtained for the Y–TZP condition, which is exclusively formed by tetragonal grains (3.9 MPa$\sqrt{m}$, see Table 2), while for the latter it may be considered as 8.0 MPa$\sqrt{m}$, following the work performed by Ingel et al. in non-transforming Y–PSZ.[34] Assuming that the total K_0 follows the law of mixtures, the values calculated using the volume fraction and the intrinsic toughness of each constituent do agree fairly good with the experimentally measured ones. Hence it may be stated that the dispersion of cubic grains toughened by tetragonal precipitates in an Y–TZP material would effectively enhance the intrinsic crack propagation resistance.

4.2. Transformation toughening

Once it is established that the microstructural changes increase the intrinsic fracture resistance, the degree of transformation toughening, which accounts for the rising R-curve detected, focuses the attention in this section. Transformation toughening in zirconia ceramics has been widely studied and exists a well-known relationship between microstructural parameters and phase transformability. For a given amount of stabilizer, the size of the tetragonal crystals determines M_S, which is intimately related with the critical stress required to activate the stress-induced phase transformation, σ_{CR}. Raising M_S up to the working temperature yields a lower σ_{CR}, which would lead to both larger transformed zones and more pronounced shielding effects around a propagating crack.[2,3,9] Accordingly, the closer the grain size distribution to d_{CR}, the larger the transformation capability exhibited by the microstructure. Lange[9] showed that in Y–TZP, d_{CR} increases with raising the stabilizer content, being 0.2 and 1 μm for 2 and 3 mol% of Y_2O_3 respectively. Such a finding is explained by the fact that d_{CR} increases as the magnitude of the change in chemical free energy is reduced.[9] Meanwhile, d_{CR} is also affected by other factors such as the matrix constraint[10] and internal residual stresses.[7,35,36] Matrix constraint is related to the elastic properties of the material surrounding the crystals of tetragonal zirconia; hence, it appears that d_{CR} should increase with the elastic modulus. This is especially interesting in microstructures where the tetragonal phase is found as precipitates (like PSZ) or as a dispersed-second phase. Internal residual stresses are usually induced by thermal expansion anisotropy or by thermal expansion mismatch in duplex microstructures.

Heat treatments at 1650°C yielded coarse-grained microstructures that allow the retention of large tetragonal grains (up to ~4 μm) at room temperature, as indicated from XRD analysis. In the 2H microstructure, tetragonal grains are present as small grains which are surrounding the larger cubic ones, being the average tetragonal grain size about 1.3 μm, but having a maximum diameter of ~4 μm. These values are quite high, specially when compared to the d_{CR} values determined for Y–TZP (varying from 0.2 to 1 μm for 2 and 3 mol% of Y_2O_3 respectively).[9] To assess that their symmetry was actually tetragonal, some Raman measurements were addressed to these grains, and the obtained spectra confirmed their tetragonality. Moreover, for the microstructure developed in 10H no monoclinic grains were detected with Raman spectroscopy. Thus, it may be postulated that the mixed microstructure developed after heat treatment permits the retention of large tetragonal grains at room temperature by increasing d_{CR}.

Although the reason for these findings is not clear, there are some aspects worthwhile considering. First, the high content of hafnia in the material (about 1.0 mol%) which may act as an additional stabilizer and induce further stabilization of the tetragonal grains.[37] Second, the reduction of the internal thermal stresses associated with less pronounced thermal mismatches.[11] For instance, Y–TZP with 2.5 mol% Y_2O_3 presents a

thermal expansion coefficient (α) about 15% higher in the c-direction than in the a-direction, in the temperature range of 1300°C to room temperature.[38] On the other hand, cubic zirconia has an isotropic value of α, which is independent of the presence of intragranular tetragonal precipitates.[39] As a result, microstructures with a larger amount of cubic phase would be expected to have less residual stresses than in a fully tetragonal microstructure with similar grain size, and consequently a corresponding higher d_{CR} would be expected. This is in complete concordance with the values of d_{CR} of about 1.5 μm resulting from combining the grain size distribution and the XRD data. This value is markedly larger than those reported by Lange in about 0.4 μm for a 2.5 mol% amount of yttria.[9]

With respect to transformation toughening, since tetragonal phase is present in the microstructure as free grains and as precipitates, it is interesting to assess the transformability of both grains and precipitates. This may shed light on the toughening mechanisms acting in the material. Then, some Raman measurements were addressed to large cubic grains broken by indentation cracks. Spectra obtained under these conditions did not show any monoclinic peak in 2H, and only some spectra revealed a very small amount of monoclinic phase in 10H. Hence, it may be stated that tetragonal precipitates were too fine to transform during crack propagation in the obtained Y–TZP/PSZ materials. This assertion is confirmed from the observations made at both flanks of the indentation crack path. Large cubic grains fractures transgranulary, whereas tetragonal grains tend to fracture in a mixed mode, that is, transgranular and intergranulary (see Fig. 8). Further, when crack propagates along the tetragonal grains, some crack closure may be observed [see Fig. 8(b)], indicating that the grain has transformed due to the crack stress field. Such closure is not observed in cubic grains, confirming that transformation is restrained to tetragonal grains while tetragonal precipitates do not transform easily.

Once it is established that the tetragonal grains are the main source of transformation toughening in these microstructures, crack shielding due to phase transformation was evaluated and compared to that obtained in R-curve experiments. The aim of such comparison was to elucidate if, as it may be anticipated, transformation toughening is the main operating mechanism in Y–TZP/PSZ materials.

Using fracture mechanics concepts, crack tip stresses may be described in terms of an applied stress intensity factor (K_{ap}). Toughening mechanisms can reduce this factor by the corresponding shielding stress intensity factor (K_S), which represents the effect of the toughening mechanisms. Hence, the effective crack-tip stress intensity factor (K_{tip}) may be expressed as:

$$K_{tip} = K_{ap} - K_S \tag{4}$$

The criterion for crack growth is that $K_{tip} = K_0$; thus, at K_{tip} values larger than K_0, the crack propagates unsteadily. K_S includes the contribution of all the toughening mechanisms, which in Y–TZP ceramics are accepted to be phase transformation and microcracking,[2–4] and the corresponding shielding are described by K_T and K_M, respectively. In the past, many efforts have been focused on relating microstructural parameters, such as the transformation zone height (h), to both K_T and K_M, yielding in equations that allow the estimation of such parameters.[2,3] Thus, assuming that the crack is fully surrounded by a transformed zone, and there is no reverse transformation, K_T may be related to the height of the transformed zone, the V_m variation along the transformed zone, and the elastic properties of the material such as the Young's modulus, E, and the Poisson's ratio, ν, according to:[2,3,18]

$$K_T = \frac{AEe^T}{(1-\nu)} \int_0^h \frac{V(y)}{2\sqrt{y}} dy \tag{5}$$

where e^T is the phase transformation strain and A is a constant depending on the morphology of the transformed

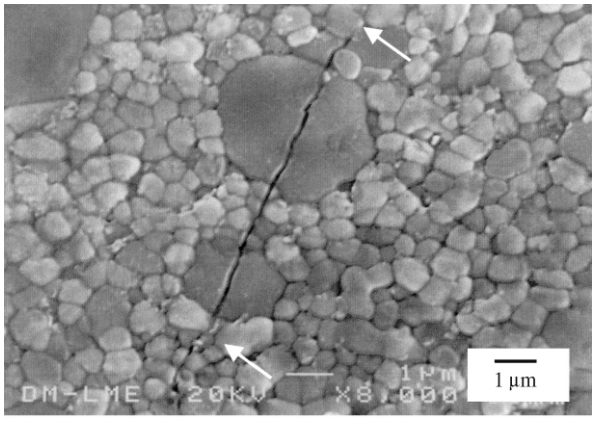

(a)

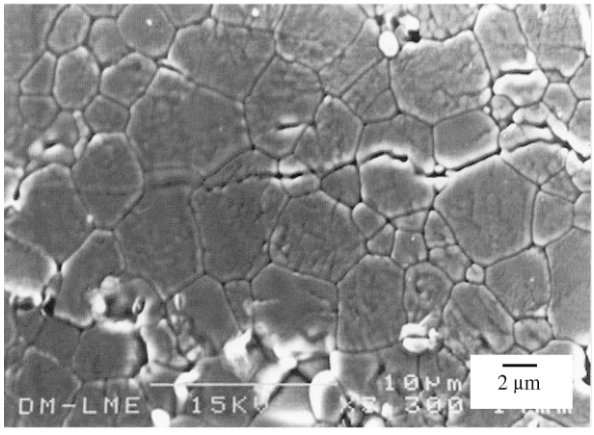

(b)

Fig. 8. Indentation crack propagation. (a) Propagation in 2H, clearly transgranular in cubic grains. (b) Transgranular propagation in 10H. In both figures it is observed some crack closure (white arrows) when crack propagates along tetragonal grains.

zone and the activation stress. If the hydrostatic stress determines h and the transformation is purely dilatational (e^T is 0.04), then the value of A is 0.22. This value may rise to 0.25 when a semicircular profile is considered.[29] Further increases may be achieved if different nucleation condition and shear strain were considered. For instance, if the transformation was activated in shear bands at 60° to the crack tip, A would be about 0.38.[3] Moreover, when transformation is initiated by the maximum principal stress and the whole transformations takes place in that direction, the value of A is 0.55.[3] Hence, the accurate evaluation of K_T involves a detailed characterization of the transformed zone.

In this work, the parameter A was calculated using the expressiion developed by Marshall,[29] combining the observed zone profiles (Fig. 7) with the assumption that phase transformation is triggered by the hydrostatic stress. It yields a value of A of 0.28 for 2H and 10H materials, meanwhile for Y–TZP, the very small transformed zone did not allow to calculate this parameter, and a value of 0.22 was chosen following the results showed in a previous work.[28]

For a reliable estimation of K_T, the key point is given by the $V_m(y)$ function. It is here where Raman spectroscopy plays a decisive role, allowing to obtain the values of V_m around cracks. In previous works, it was proposed to use an expression like $V_m(y) = a - by^{1/2}$,[18] but with this expression it was not possible to fit well the experimental results. Therefore, special attention was paid in this study to find a better fitting approach. The best function found is expressed by Eq. (6), where b is a fitting parameter, calculated to be 13.1±1.9 for 2H, and 17.0±1.7 for 10H, with excellent χ^2 coefficients (0.00002). Experimental results of $V_m(y)$ and this fitting are shown in Fig. 9.

$$V(y) = \frac{V_F}{1 + b\left(\frac{y}{h}\right)^2} \tag{6}$$

where V_F is the monoclinic amount found in the fracture surfaces. Combining Eqs. (5) and (6) the value of

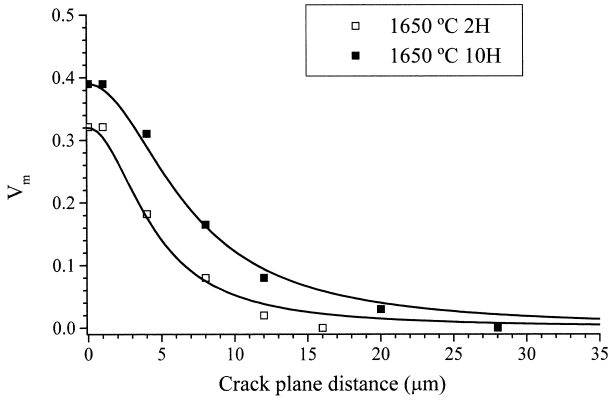

Fig. 9. Variation of V_m along the transformed zone.

K_T was calculated, assuming that transformation is purely dilatational and all the shear strains are relieved by twinning ($e^T = 0.04$, A values as given in Table 3). The values of E and ν used were 200 GPa and 0.3 respectively.[4]

The estimated shielding is shown in Table 4, where it can be seen that it differs slightly from the experimental values of K_S. Such differences are not unusual, and some examples may be found in the open literature. For example, moderate to large differences in estimated with respect to observed transformation toughening are commonly reported for Mg–PSZ, when calculations are based on the assumption that transformation is purely dilatant (see for example Refs. 5 or 18). However, the experimental results obtained here are quite close to the calculations. One reason for these small discrepancies may be that the R-curve was measured using ideal semielliptical cracks, which are thought to give a very accurate measure of the transformation toughening. Evaluations of the R-curve with other crack systems, as for example indentation cracks, would result in an overestimation of the crack shielding, due to the presence of the uncracked ligament, bridging crack surfaces.[30]

The reason for the differences still remaining between estimated and obtained shielding may be the consequence of partial reversibility in the transformation, shear contribution to the transformation strain and/or the existence of other toughening mechanisms. Some studies suggested that a shear component may exist in regions close to the crack tip, and this deformation should be added to e^T to obtain the total amount of transformation toughening.[40] One of the active secondary toughening mechanism could be associated with some interactions between tetragonal precipitates/cubic matrix and the crack. Similarly to the crack bridging discerned, for example, in Mg–PSZ materials between propagating cracks and large precipitates.[31,32] However, in Y–TZP/PSZ materials, tetragonal precipitates are too fine, and the extension of bridging that they could produce is possibly too small to be relevant for their contribution to toughness. Another toughening mechanism that may take place is microcracking associated with phase transformation.[41] It is known that transformed monoclinic particles are surrounded by microcracks due to volumetric expansions. From this viewpoint, the formation of a microcracked zone around a propagating

Table 4
Crack shielding obtained from R-curve measurements (K_S) and estimated shielding due to phase transformation (K_T) and microcracking (K_M)

Material	K_S (MPa$\sqrt{m}$)	K_T (MPa$\sqrt{m}$)	K_M (MPa$\sqrt{m}$)
Y–TZP	0.4	0.2	–
2H	2.4±0.2	1.8±0.4	0.6±0.1
10H	3.0±0.3	2.8±0.2	0.9±0.2

crack would reduce the crack tip stress and induce shielding[41]. The source for this toughening comes from the residual opening of the microcracks that produces compressive stresses. Formally, it may be analyzed following similar steps to those used for phase transformation toughening, and the associated toughening increment (K_M) may be quantitatively described by Eq. (5). In order to get an idea of the contribution of microcracking to shielding, a calculation may be performed, using simple approaches to describe this mechanism. Faber suggested that the strain related to microcracking, e^M, associated with a transformed particle of volume V, may be expressed as:[41]

$$e^M = \frac{2e^T}{3}\left[V + \left(\frac{3V}{4\pi}\right)^{1/3}\right] \quad (7)$$

Inserting Eq. (7) into Eq. (5), K_M may then be calculated assuming that V is a function of the distance to the crack flank and follows Eq. (6). The obtained results of K_M are listed in Table 4. The smaller values of K_M compared to those of K_T provide additional reasons for describing microcracking as a secondary mechanism, and it may possibly account for the observed shielding as well.

Finally, since results given in Tables 4 and 5 have clearly shown that heat treatments at 1650°C enhance the transformation capability of the developed Y–TZP/PSZ, its transformability was compared to that of microstructures with a well-known degree of transformation, i.e. Ce–TZP[8,29] and Mg–PSZ materials.[5] The parameter which give an idea of the feasibility of the stress-induced transformation is σ_{CR}. At a given temperature, low σ_{CR} indicates that the material can transform easily. Applying fracture mechanics concepts, σ_{CR} may now be obtained from the values of h and K_0. If phase transformation is triggered by the hydrostatic stress, σ_{CR} may be obtained from:

$$\sigma_{CR} = \sqrt{\frac{\sqrt{3}}{12\pi}}\frac{K_0(1+\nu)}{\sqrt{h}} \quad (8)$$

Using the values of h and K_0 (Tables 2 and 3), σ_{CR} was calculated for each microstructure and the results are shown in Table 5. Further, the transformability parameters for two Ce–TZP materials are included in this table. One of these materials has a grain size comparable to the present 10H microstructure (material Ce–TZP–A, h about 40 μm and K_T of 6 MPa$\sqrt{m}$) and other has a coarser microstructure (material Ce–TZP–B, mean grain size of 8 μm, h about 300 μm and K_T of 14 MPa$\sqrt{m}$).[8] For similar comparison purposes, the transformation properties for two Mg–PSZ materials are also shown in Table 5 (Mg–PSZ–A, with $h = 9$ μm and $K_T = 3.0$ MPa$\sqrt{m}$ and Mg–PSZ–B, with $h = 65$ μm and $K_T = 4.0$ MPa$\sqrt{m}$).[5] The microstructure transformability of 2H is similar to that exhibited by Mg–PSZ-A; although crack shielding is noticeably smaller. The transformation properties of 10H are similar to those obtained for Ce–TZP–A, but transformation toughening is more pronounced in Ce–TZP–A. High toughness Ce–TZP and Mg–PSZ (Ce–TZP–B and Mg–PSZ–B) offer much higher fracture toughness values.

However, the interest in the here-developed Y–TZP/PSZ materials is the concomitant high values of the fracture strength and toughness (Table 2). The reported fracture strength (for prismatic bars under four-point bending) of the above mentioned high toughness ceramics are about 400 MPa for Ce-TZP[42] and 464 MPa for Mg–PSZ.[31] These values are clearly smaller than those obtained for the present mixed Y–TZP/PSZ microstructures. Although such high strength is usually obtained in fine-grained Y–TZPs, produced by sintering at low temperatures, fracture toughness in these materials may be described as rather low. Thus, heat treatment of fine-grained Y–TZPs at 1650°C for moderate times (about 2 h) seems to be a promising way to get a zirconia ceramic that combine high fracture strength with quite large fracture toughness.

5. Conclusions

Microstructural changes promoted in Y–TZP via heat treatment at 1650°C were accurately studied, using XRD and Raman microprobe spectroscopy. Crack propagation resistance of the resulting microstructures was evaluated and related to transformation capability as well as to microstructural differences. From these results, the following conclusions can be drawn:

1. Heat treatments of a 2.5 mol% yttria-stabilized zirconia at 1650°C result in a pronounced change in the microstructure. It evolves from an initially

Table 5
Transformability of each microstructure, in terms of transformation activation stresses (σ_{CR}). Reported values for various Ce–TZP[8,29] and Mg–PSZ materials[5] are also included for comparison

Material	Y–TZP	2H	10H	Ce–TZP A	Ce–TZP B	Mg–PSZ A	Mg–PSZ B
σ_{CR} (MPa)	630	350	305	350	161	471	171

fine-grained Y–TZP to an aggregate of cubic grains surrounded by tetragonal grains. In the cubic grains, a dispersion of very fine tetragonal precipitates was found. Since the obtained microstructures exhibit features close to both Y–TZP and PSZ they are termed as mixed Y–TZP/PSZ ceramics.

2. The obtained microstructures allow the retention of large tetragonal grains (up to ~4 μm). Since transformation of these grains into monoclinic symmetry is now more favorable than for conventional Y–TZP, phase transformability is enhanced. This raises the shielding effects developed by t→m transformation, resulting in a pronounced R-curve behavior.
3. Determination of the transformed zone height by Raman microprobe spectroscopy showed that the developed Y–TZP/PSZ materials extensively experience t→m phase transformation around a propagating crack with large values of transformed zone heights, 16 and 28 μm for 2H and 10H respectively.
4. Transformed zone tip profiles around an indentation crack were semicircular in Y–TZP/PSZ materials, similar to transformed zone profiles detected in high-toughened Mg–PSZ ceramics.
5. Estimation of transformation toughening was made using the dimensions and morphology of transformed zones as well as the monoclinic phase distribution found along them and assuming only dilatant transformation. The obtained shielding does practically agree with experimental results of crack shielding attained in R-curve measurements. The differences could be minimized if shear contributions are accounted, or by assuming that there is some contribution to toughening from microcracking. Thus, the t→m transformation is identified as the main operating mechanism in Y–TZP/PSZ materials.
6. The more interesting feature of the developed Y–TZP/PSZ materials is the combination of high fracture strength (similar to that of fine-grained Y–TZP) and relatively high fracture toughness (close to that typical of Mg–PSZ and Ce–TZP), which is not usually found in highly transformable ceramics, as Ce–TZP and Mg–PSZ.

Acknowledgements

This investigation has been partly supported by the Generalitat de Catalunya under grant number 1999SGR00129 and by the Spanish CICYT under Grant number MAT97-0923. One of the authors (D.C.) is grateful to Generalitat de Catalunya for financial support through an FI scholarship. It is also a pleasure to thank the helpful discussions with J. Alcalá. Finally, R. Warren is kindly acknowledged for useful comments and for providing the opportunity of using experimental facilities at Luleå University of Technology.

References

1. Garvie, R. C., Hannink, R. H. and Pascoe, R. T., Ceramic steel? *Nature (London)*, 1975, **258**, 703–704.
2. McMeeking, R. and Evans, A. G., Mechanics of transformation toughening in brittle materials. *J. Am. Ceram. Soc.*, 1982, **65**, 242–250.
3. Evans, A. G. and Cannon, R. N., Toughening of brittle solids by martensitic transformations. *Acta Metall.*, 1986, **34**, 761–800.
4. Green, D. J., Hannink, R. H. J. and Swain, M. V., *Transformation Toughening of Ceramics*. CRC Press Inc, Florida, 1989.
5. Hannink, R. H. J., Howard, C. J., Kisi, E. H. and Swain, M. V., Relationship between fracture toughness and phase assemblage in Mg–PSZ. *J. Am. Ceram. Soc.*, 1994, **77**, 571–579.
6. Swain, M., Grain-size dependence of toughness and transformability of 2 mol% Y–TZP ceramics. *J. Mater. Sci.*, 1986, **5**, 1159–1162.
7. Becher, P. F. and Swain, M. V., Grain-size-dependant transformation behavior in polycrystalline tetragonal zirconia. *J. Am. Ceram. Soc.*, 1992, **75**, 493–502.
8. Becher, P. F., Alexander, K. B., Bleier, A., Waters, S. B. and Warmick, H., Influence of ZrO_2 grain size and content on the transformation response in the Al_2O_3–ZO_2 (12 mol% CeO_2) system. *J. Am. Ceram. Soc.*, 1990, **76**, 657–663.
9. Lange, F. F., Transformation toughening. *J. Mater. Sci.*, 1986, **17**, 225–246.
10. Garvie, R. C. and Swain, M. V., Thermodynamics of the tetragonal to monoclinic phase transformation in constrained zirconia microcrystals. *J. Mater. Sci.*, 1985, **20**, 1193–1200.
11. Ruiz, L. and Readey, M. J., Effect of heat treatment on grain size, phase assemblage, and mechanical properties of 3 mol% Y–TZP. *J. Am. Ceram. Soc.*, 1996, **79**, 2331–2340.
12. Scott, H. G., Phase relationships in zirconia-yttria system. *J. Mater. Sci.*, 1975, **10**, 1527–1535.
13. Rühle, M., Claussen, N. and Heuer, A. H., Microstructural studies of Y_2O_3-containing tetragonal ZrO_2 polycrystals (Y–TZP). In *Advances in Ceramics: Science and Technology of Zirconia II*, ed. N. Claussen, M. Rühle and A. H. Heuer. Am. Ceram. Soc., Columbus, OH, 1984, pp. 352–370.
14. Govila, R. K., Strength characterization of yttria-partially-stabilized zirconia. *J. Mater. Sci.*, 1995, **30**, 2656–2667.
15. Phillippi, C. M. and Mazdiyasni, K. S., Infrared and Raman spectra of zirconia polymorphs. *J. Am. Ceram. Soc.*, 1971, **54**, 254–258.
16. Keramidas, V. G. and White, W. R., Raman scattering study of the crystallisation and phase transformations of ZrO_2. *J. Am. Ceram. Soc.*, 1974, **57**, 22–24.
17. Clarke, D. R. and Adar, F., Measurement of the crystallographically transformed zone produced by fracture in ceramics containing tetragonal zirconia. *J. Am. Ceram. Soc.*, 1982, **65**, 284–288.
18. Marshall, D. B., Shaw, D. C., Dauskardt, R. H., Ritchie, R. O., Readey, M. J. and Heuer, A. H., Crack-tip transformation zones in toughened zirconia. *J. Am. Ceram. Soc.*, 1990, **73**, 2659–2666.
19. Casellas, D., Alcalá, J., Llanes, L. and Anglada, M., Fracture variability and R-curve behavior in yttria-stabilized zirconia ceramics. *J. Mater. Sci.*, in press.

20. Cumbrera, F. L., Sánchez-Bajo, F., Fernández, R. and Llanes, L., Microstructure effects in the X-ray powder diffraction profile of 9 mol% Mg–PSZ. *J. Eur. Ceram. Soc.*, 1998, **18**, 2247–2252.
21. Heuer, A. H., Lanteri, V. and Domínguez-Rodríguez, A., High temperature precipitation hardening of Y_2O_3 partially stabilized ZrO_2 (Y–PSZ) single crystals. *Acta Metall.*, 1989, **37**, 559–567.
22. Matsui, M., Soma, T. and Oda, I., Effects of microstructure on the strength of Y–TZP components. In *Advances in Ceramics: Science and Technology of Zirconia II*, ed. N. Claussen, M. Ruhle and A. H. Heuer. Am. Ceram. Soc., Columbus, OH, 1984, pp. 371–380.
23. Sakuma, T., Yoshizawa, Y.-I. and Suto, H., The modulated structure formed by isothermal aging in ZrO_2–5.2 mol% Y_2O_3. *J. Mater. Sci.*, 1985, **20**, 1085–1092.
24. Zhou, Y., Ge, L., Lei, T. C. and Sakuma, T., Diffusional cubic-to-tetragonal phase transformation and microstructural evolution in ZrO_2–Y_2O_3 ceramics. *J. Mater. Sci.*, 1991, **26**, 4461–4467.
25. Dauskardt, R. H., Kink, D. and Ritchie, D. O., Spatially resolved raman spectroscopy study of transformed zones in magnesia-partially-stabilized zirconia. *J. Am. Ceram. Soc.*, 1989, **72**, 1124–1130.
26. Behrens, G., Dransmann, G. W. and Heuer, A. H., On the isothermal martensitic transformation in 3Y–TZP. *J. Am. Ceram. Soc.*, 1993, **76**, 1025–1030.
27. Stanley, P., Fessler, H. and Sivill, A. D., The unit strength concept in the interpretation of beam test results for brittle materiales. *Proc. Instn. Mech. Engrs.*, 1976, **190**, 585–595.
28. Anderson, R. M. and Braun, L. M., Technique for the R-curve determination of Y–TZP using indentation-produced flaws. *J. Am. Ceram. Soc.*, 1990, **73**, 3059–3062.
29. Marshall, D. B., Crack shielding in ceria-partially-stabilized zirconia. *J. Am. Ceram. Soc.*, 1990, **73**, 3119–3121.
30. Alcalá, J. and Anglada, M., Indentation precracking of Y–TZP: implications to R-curves and strength. *Mat. Sci. and Eng.*, 1998, **A245**, 267–276.
31. Fernández, R., Casellas, D., Cumbrera, F.L, Sánchez-Bajo, F., Anglada, M. and Llanes, L., Phase assemblage effects on the fracture and fatigue characterization of magnesia-partially stabilized zirconia. *Int. J. Ref. Met. Hard Mater.*, 1998, **16**, 291–301.
32. Hoffman, M. J., Lenz, W., Swain, M. V. and Mai, Y.-W., Cyclic fatigue lifetime predictions of partially stabilized zirconia with crack resistance curve characteristics. *J. Eur. Ceram. Soc.*, 1993, **11**, 445–453.
33. Michel, D., Mazerolles, M. and Perez, M. Polydomain crystals of single-phase tetragonal ZrO_2: structure, microstructure and fracture toughness. In *Advances in Ceramics: Science and Technology of Zirconia II*, ed. N. Claussen, M. Ruhle and A.H. Heuer. Am. Ceram. Soc., Columbus, OH, 1984, pp. 131–138.
34. Ingel, R. P., Rice, W., Bender, B. A. and Lewis, D., Physical, microstructural, and thermomechanical properties of ZrO_2 single crystals. In *Advances in Ceramics: Science and Technology of Zirconia II*, ed. N. Claussen, H. Rühle and A. H. Heuer. Am. Ceram. Soc., Columbus, OH, 1984, pp. 408–414.
35. Schmauder, S. and Schubert, H., Significance of internal stresses for the martensitic transformation in yttria-stabilized tetragonal zirconia polycrystals during degradation. *J. Am. Ceram. Soc.*, 1986, **69**, 534–540.
36. Schubert, H. and Petzow, G., Microstructural investigations on the stability of yttria-stabilized tetragonal zirconia. In *Advances in Ceramics Vol. 24A: Science and Technology of Zirconia III*, ed. S. Somiya, N. Yamamoto and H. Yanagida. Am. Ceram. Soc., Columbus, OH, 1986, pp. 21–28.
37. Kim, D.-J., Effect of Ta_2O_5, Nb_2O_5, and HfO_2 alloying on the transformability of Y_2O_3-stabilised tetragonal ZrO_2. *J. Am. Ceram. Soc.*, 1990, **73**(1), 115–120.
38. Schubert, H., Anisotropic thermal expansion coefficients of Y_2O_3 stabilized tetragonal zirconia. *J. Am. Ceram. Soc.*, 1986, **69**, 270–271.
39. Adams, J. W., Nakamura, H. H., Ingel, R. P. and Rice, R. W., Thermal expansion behavior of single-crystal zirconia. *J. Am. Ceram. Soc.*, 1985, **68**, 228–231.
40. Cox, B. N. and Marshall, D., Surface displacement analysis of the transformed zone in magnesia-partially stabilized zirconia. *J. Eng. Mater. Technol.*, 1988, **110**, 105–119.
41. Faber, K. T., Microcracking contributions to the toughness of ZrO_2-based ceramics. In *Advances in Ceramics: Science and Technology of Zirconia II*, ed. N. Claussen, M. Ruhle and A. H. Heuer. Am. Ceram. Soc., Columbus OH, 1984.
42. Readey, M. J. and McCallen, C. L., Microstructure flaw tolerance, and reliability of Ce–TZP and Y–TZP ceramics. *J. Am. Ceram. Soc.*, 1995, **78**, 2769–2776.